Large eddy simulation of buoyant jet in shallow water

Akihiko Nakayama, Jeremy D. Bricker and Zafarullah Nizamani

Department of Environmental Engineering,
Universiti Tunku Abdul Rahman
akihiko@utar.edu.my

Abstract

A numerical method of predicting the turbulent mixing process of disposed water from an outfall in a shallow coastal water is described. The momentum equations for the sea water mixed with treated water of small salinity and warmer temperature are solved numerically together with the equation of the concentration of the treated water. The basic method is a Large Eddy Simulation (LES) formulated on a fixed rectangular grid where boundaries are approximated by Immersed Boundary (IB) method. The sub-grid effects of the unresolved fluctuations of velocity and the concentration fields are expressed by the eddy viscosity and eddy diffusivity with the Smagorinsky model. The method is verified with an experiment and RANS calculation of the buoyant wall jet issuing on a solid surface. The method then is used to simulate the dispersion and dilution of the effluent from a typical marine outfall installed on the seabed of shallow coastal water. The behavior of the plume in the vicinity of the outfall is simulated well reproducing the dilution process and the surface boil.

1 Introduction

It is important that the disposal of treated waste water is done properly anywhere, but is more so when it has to be done near a large city with many activities influenced by the quality and the temperature of sea water along the coast. While high water quality may be achieved by advanced treatment methods, the control of the temperature of the treated water is difficult and requires an expensive facility like a cooling pool. Therefore, an accurate estimate of the dispersion of the disposed water is required for the planning and operating a treatment plant.

There are a number of methods that may be used to predict the spread and dilution of the effluent concentration. A rough estimate may be made by using a method based on simple integral models (Blumeberg and Mellor, 1987). An estuary model (Nakatsuji et al., 1992) or regional ocean simulation models such as CORMIX (Donecker and Jirka, 2007) and ROMS (Buijsman et al., 2012) can also be used to obtain detailed distribution of contamination. These methods are based on the Reynolds-averaged equations of motion and the diffusion equation for contaminant transport that require appropriate turbulence models. Turbulence models in situations where the local fluid motion and mixing are influenced by complex bathymetry with coastal structures and buoyancy due to salinity or temperature differences are not accurate or reliable. Also they are meant to predict the behavior of the dispersion in the far field after the

effluent has spread to the full depth of the sea.

Large Eddy Simulation (LES) methods simulate the large-scale motion directly that are responsible for mixing and transports of the mixed fluid by modeling small-scale fluctuations and are more suited for dispersion calculations in complex geometry and boundary conditions. The main problem is the large calculation loads. Here we apply an LES method with a wall model so the near field dispersion of contaminant can be simulated with a computational grid of a reasonable size without resolving the viscosity influenced bottom layer. The detailed three dimensional distributions of the concentration and the temperature in the near field extending over a few hundred meters from the outfall can still be obtained.

In the following, first the basic equations to simulate the motion of seawater mixed with fresh water of small salinity and different temperature are described in the framework of the large eddy simulation with the necessary models. Then a brief description of the numerical method used to solve them is given. The method is validated in calculation of a basic buoyant jet Figure 1) before applying to an outfall dispersion in real case.

2 Computational Method

The basic equations we solve are the spatially-filtered equations of motion with Boussinesq approximation

$$\frac{\partial u_i}{\partial t}+\frac{\partial (u_i u_j)}{\partial x_j}+2\varepsilon_{ijk}\Omega_j u_k=-\frac{1}{\rho_0}\frac{\partial p}{\partial x_i}+\nu\frac{\partial^2 u_i}{\partial x_j \partial x_j}-\delta_{i3}\big(\beta(T-T_0)+\zeta(C-C_0)\big)g-\frac{\partial \tau_{ij}}{\partial x_j} \quad (1)$$

$$\frac{\partial u_i}{\partial x_i}=0 \quad (2)$$

Here u_i is the velocity component in x_i direction, Ω_j is the earth's rotation vector, T_0 and C_0 are the ambient temperature and the ambient concentration of the treated water, p is the pressure, ν is the coefficient of the kinematic viscosity, β and ζ are the coefficient of thermal expansion of the water due to the changes of temperature and concentration from the reference values T_0 and C_0 at which the water density is ρ_0, g is the acceleration due to gravity, τ_{ij} is the sub-grid stress components and x_i is the Cartesian coordinates with x_3 (which may be designated by z) vertically upward direction. The sub-grid stress τ_{ij} in the present calculation is modeled by the standard Smagorinsky model

$$\tau_{ij}=\nu_{sgs}\left(\frac{\partial u_i}{\partial x_j}+\frac{\partial u_j}{\partial x_i}\right), \qquad \nu_{sgs}=(C_S\Delta)^2\left|\frac{1}{2}\left(\frac{\partial u_i}{\partial x_j}+\frac{\partial u_j}{\partial x_i}\right)\left(\frac{\partial u_i}{\partial x_j}+\frac{\partial u_j}{\partial x_i}\right)\right|^{1/2}, \quad (3), (4)$$

with Smagorinsky constant C_S=0.11 and the average grid spacing for Δ.

The boundary conditions to be used for these equations make use of the wall similarity law for the solid wall boundary condition. In other words, the shear stress on solid walls is

calculated by the following model equation and is used in the momentum equation instead of using (3).

$$\tau_{ij} = C_d \rho V_1 u_{tj1} \tag{5}$$

Here the subscript 1 means the value at the computational point closest to the sold wall and $V_1 = \sqrt{u_1^2 + v_1^2 + w_1^2}$ is the total velocity and u_{tj} is the component of the tangential velocity in x_j direction there and C_d is the resistance coefficient determined from the standard wall similarity law for smooth or rough surfaces using V_1 and the distance from the wall y_1. This way the no-slip velocity condition, which is a poor approximation for high Reynolds number flows with coarse grid, is not used. This is important since the simulation will be conducted for flows with the dimensions of the real coastal water.

The equations for the filtered water temperature T and the filtered concentration C of the treated water are

$$\frac{\partial T}{\partial t} + \frac{\partial (T u_j)}{\partial x_j} = \alpha \frac{\partial^2 T}{\partial x_j \partial x_j} - \frac{\partial q_j}{\partial x_j} \tag{6}$$

$$\frac{\partial C}{\partial t} + \frac{\partial (C u_j)}{\partial x_j} = \gamma \frac{\partial^2 C}{\partial x_j \partial x_j} - \frac{\partial h_j}{\partial x_j} \tag{7}$$

where α and γ are the coefficients of the heat conduction and the concentration diffusion which are assumed constant, q_j and h_j are the sub-grid heat flux and the sub-grid flux of the concentration, which are modeled by the sub-grid eddy diffusivity model with the eddy diffusivity coefficient determined by an extension of the Smagorinsky model.

$$q_j = \frac{\nu_{sgs}}{\sigma_{sgs}} \frac{\partial T}{\partial x_j} \quad , \quad h_j = \frac{\nu_{sgs}}{\sigma_{sgs}} \frac{\partial C}{\partial x_j} , \tag{8), (9}$$

The value of the sub-grid diffusion Prandtl number σ_{sgs} is assumed to be constant 0.7 and no modification for the effects of stratification are used since the large eddies that are influenced more than the modeled small-scale motions by the buoyancy are directly calculated in LES.

The water surface is expressed by its elevation h as a function of the horizontal coordinates (x_1, x_2) or (x, y). It is determined by solving the kinematic boundary condition

$$\frac{\partial h}{\partial t} + \frac{\partial (h u_{s1})}{\partial x_1} + \frac{\partial (h u_{s2})}{\partial x_2} = u_{s3} + \frac{\partial \tau_{hx}}{\partial x_1} + \frac{\partial \tau_{hy}}{\partial x_2} \tag{10}$$

where (u_{s1}, u_{s2}, u_{s3}) are the velocity components on the free surface and τ_{hx}, τ_{hy} are the sub-grid free-surface fluctuation terms (Hodges & Street, 1999), which we model by the gradient model

(Yokojima & Nakayama, 2002).

In general, the large-eddy simulation with the resolution of the order of a few million grid points appear to represent mixing and dispersion processes without explicitly modelling the buoyancy effects. This is because the motion of the large eddies are simulated directly with the buoyancy and stratification effects and the large eddies are the motion that is mostly responsible for the overall mixing and dispersion

3 Calculation of buoyant wall jet in water at rest

First the dispersion of hot water injected into ambient still cold water is calculated. The hot water jet is issued horizontally through a circular tube of negligible wall thickness placed on the bottom floor of a mixing basin as shown in Figure 1.

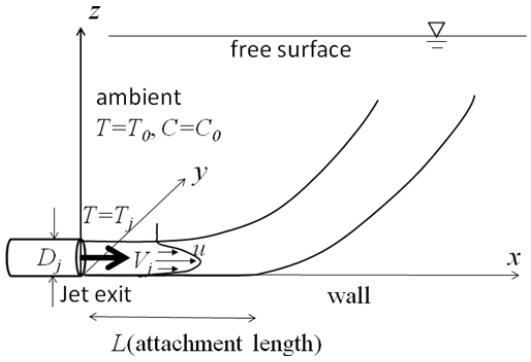

Case	D_j (mm)	V_j (mm/s)	T_j (deg)	T_a (deg)	F_d	Re_j	L/D_j
Case1	4.7	1.0	60	20	37.7	10086	119
Case2	4.7	1.75	90	20	44.2	26111	149

Figure 1. Buoyant jet issuing from a circular pipe on a wall.

The temperature and the density of the issuing water are T_j and ρ_j, respectively. The mean velocity of the jet at the exit is V_j. The diameter of this jet is D_j and the temperature and the density of the ambient water are T_0 and ρ_0, respectively. The depth of the water in the experiment is large compared with the jet diameter and the free surface condition is not needed. The rest of the calculation conditions are taken the same as the experiment of Sharp & Vyas (1977) and the numerical calculation by Huai et al. (2010) and are summarized in Table 1. The Reynolds number Re_d indicated in the table is defined by D_j, V_j and the kinematic viscosity ν which is assumed to be constant. The Froude number F_d is defined by $F_d = V_j / \sqrt{gD_j(\rho_0 - \rho_j)/\rho_j}$. L shown in Figure 1 is the attachment length defined by the

horizontal distance from the jet exit to the point where the temperature dilution ratio $S=(T-T_0)/(T_j-T_0)$ becomes 0.03 on the wall.

Calculations for two cases with different Reynolds and Froude numbers are conducted. In these validation cases, the density is a sole function of the temperature and the concentration C of the jet fluid does not directly influence the flow. In the numerical calculation, a rectangular grid of constant spacing is used. The grid spacing in the horizontal directions is 2mm and that in the vertical direction is 1mm, so the jet exit cross section is represented by 4 x 2 cells and the volume discharge rate rather than the point-wise velocity is set to correspond to the experiment. The total of 79 x 67 x 82 grid points are used to cover the region of 200 diameters in the horizontal direction and 30D in the depth direction. The horizontal distance in the direction of the jet is sufficiently large so the boundary condition at the right boundary does not influence the plume trajectory.

The calculation results are shown in Figures 2 and 3. Figure 2(a) shows the velocity distribution in two planes perpendicular to the jet axis in the near field close to the exit. They verify the velocity calculation by comparing with Verhof's theoretical solution. The velocity is normalized by the average velocity U_m across the jet cross section and the height $z_{1/2}$ where the velocity is one half of the maximum. The shape of the distribution above the near wall layer agrees with Verhof's profile. The Verhof used the inviscid assumption and the velocity is made to have zero slope on the wall which is not realistic. In the present calculation, the wall model based on the wall similarity is used. Figure 2(b) shows the calculated attachment length L of the two calculation cases compared with the experiments of Sharp & Vyas (2007) and the RANS calculation of Huai et al. (2010). It is seen that the calculation results are slightly smaller than the experiment but the trend agrees with the mean of the experimental values. The present results are only near the high end of the Froude number range of the experimental data but are seen to agree with them and the RANS calculation.

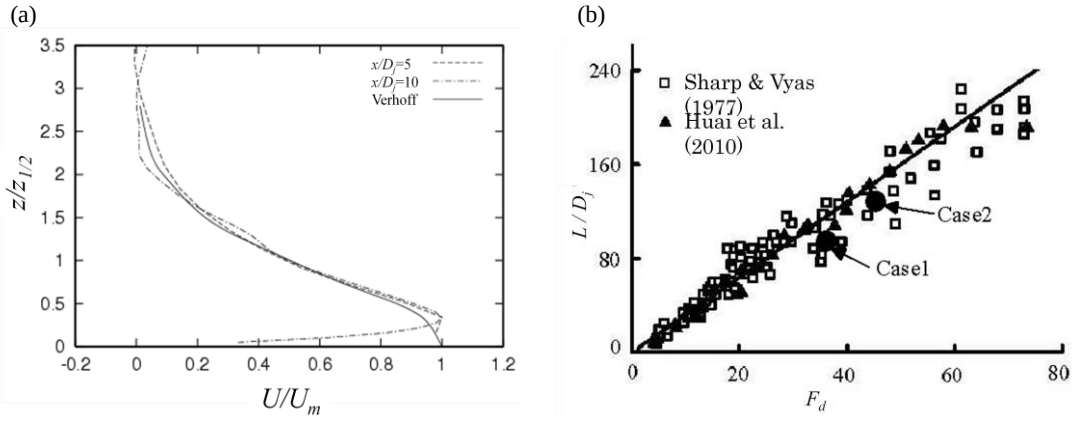

Figure 2. The calculated mean velocity distribution in attached region and attachment length compared with experiments.

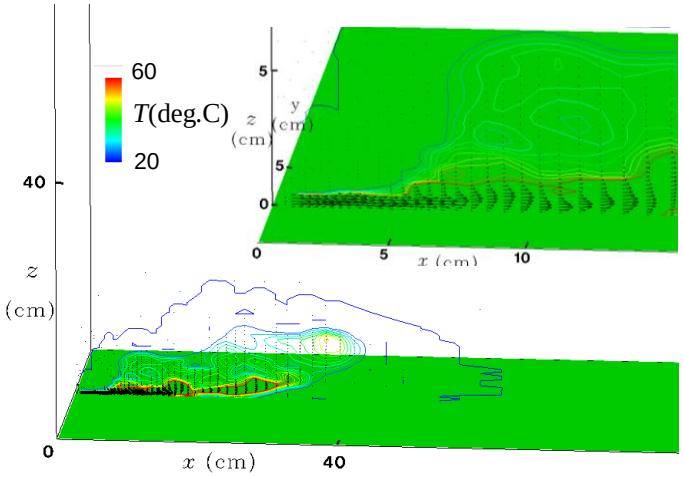

Figure 3. The instantaneous velocity and temperature distributions. Upper right inset is the enlarged view near the jet exit.

Figure 3 is the snapshots of instantaneous distributions of the velocity vectors and the temperature distribution in the vertical plane through the jet axis. The upper inset is the enlarged view near the exit. The way the buoyant effluent billows up is seen to be reproduced well.

4 Calculation of initial dispersion from a real outfall

Figure 4 shows a numerical representation of a coastal water zone where treated water is disposed from an outfall placed on the sea bed. An underground pipe runs from the bottom of the plant transporting the treated water to the seabed where the outfall ports are installed. The average depth of the water is 12m and the location of the outfall is 20m offshore from the seawalls. We simulate the initial mixing of the treated water discharged from 6 discharge nozzles directed in the horizontal direction. The objective is to obtain the detailed concentration variation of the treated water and the temperature rises in the vicinity of the plant.

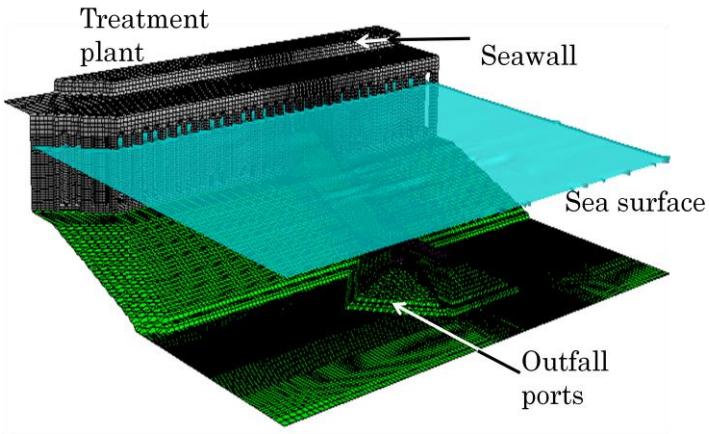

Figure 4. Water treatment plant outfall on seabed along a coast.

It is assumed that there are tidal currents with varying velocity and direction depending on the tidal phase. The computational grid is rectangular as in the validation case, but the grid spacing in the horizontal directions is now variable. The smallest horizontal spacing is 25cm near the outfall ports and 4m at the outer boundaries. The vertical grid spacing is 10cm with 48 grids in the vertical directions. The calculation region is 700m x 1000m x 15m in the offshore, alongshore and depth directions, respectively covered by 182 x 214 x 48 grid points. The outlet nozzle cross section of the outfall port is resolved by 2 x 2 cells.

Figure 5 shows the instantaneous flow and the temperature fields for the Case A and Case B with two different current directions in a vertical plane passing through the center of the outfall ports. Figure 5(a) is the case when the tidal current is in the direction of the outfall nozzles and Figure 5(b) is the case when the current opposes the direction of the outfall.

In both cases, the treated water has initial salinity zero and the temperature 2.0 degrees higher than the sea water. The plume rises within a short distance from the outfall ports and forms a boil on the sea surface. After the plume reaches the surface it rapidly spreads in the horizontal directions. It is what usually is observed at the sites of in shallow disposals.

(a) Case A, westward current

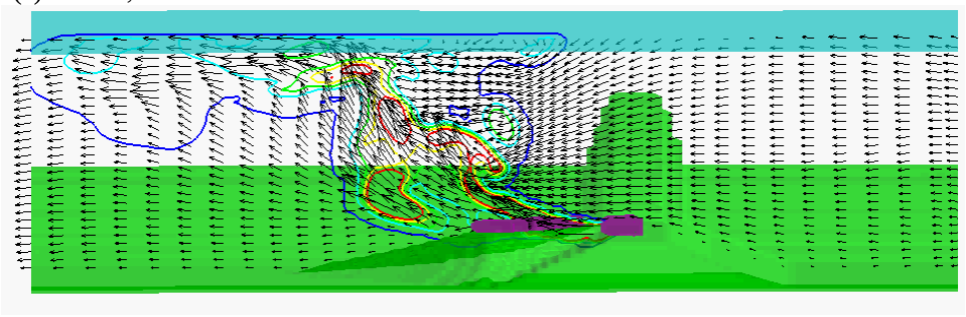

(b) Case B, eastward current

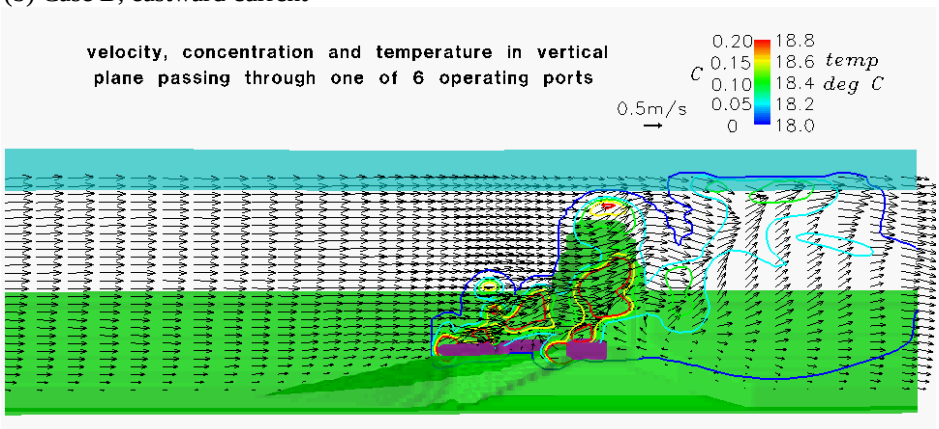

Figure 5. Simulation of buoyant effluent disposed in a shallow coastal water.

5 Conclusion

The large eddy simulation method based on the filtered equations of Boussinesq approximated equations of motion for the treated water mixed in the ambient sea water has been developed. After it is validated in the calculation of basic buoyant jets it is applied to simulate the dispersal of a model case of a treated water marine disposal. It does not make hydrostatic or other approximations and resolve the turbulent motion responsible for the mixing processes and is able to simulate the detailed mixing and dispersal processes in the region close to the outfall. Although there is a limitation on the extent of the simulation region and the duration of the simulation period, it can be improved as the computer performance is improved. The present method can be an alternative to integral methods that make drastic assumptions like Gaussian distribution.

References

Blumeberg, A. F. and Kantha, I. H. (1985). Open boundary condition for circulation models, *J. Hydraul. Eng*., 111(2), 237-255.

Blumeberg, A. F. and Mellor, G. L. (1987). A description of a three-dimensional coastal ocean circulation model. *Three-Dimensional Coastal Ocean Models.* Ed., N. S. Heaps, Vol. 4, Coastal and Estuarine Sciences, Amer. Geophys. Union, 1–16.

Bricker, D.J., Nakayama, A. Aoki, C. and Takada, M. (2006). Plume tracing in the coastal area with strong tidal currents, *JSCE Journal of Coastal Engineering*, 53, 346-350 .

Bujisman, M., Uchiyama, Y., McWilliams, J.C. and Hill-Lindsay, C.R. (2012). Modeling semiduirnal internal tides in the Sourthern California Bight, *J. Phys. Oceanogr.*, 42, 62-77.

Donecker, R.L. and Jirka, G.H. (2007). CORMIX User Manual: A Hydrodynamic Mixing Zone Model and Decision Support System for Pollutant Discharges into Surface Waters, EPA-823-K-07-001.

Frick, W.E., Roberts, P.J.W., Davis, L.R., Keyes, J., Baumgartner, J. and George, K.P. (2003). Dilution models for effluent discharges, 4th ed., U.S. Environmental Protection Agency, Washington.

Hirt, C.W. and Cook, J.L. (1972). Calculating three-dimensional flow around structure and over rough terrain. *J. Comput. Phys.* 10, 324–340.

Hodges, B.R. and Street, L. R. (1999). On simulation of turbulent nonlinear free-surface flows, *J. Comp. Phys*. 151, 425-457.

Huai, W.-X., Li, Z.-W., Qian, Z.-D., Zeng, Y. and Hann, J. (2010). Numerical simulation of horizontal buoyant wall jet, *Journal of Hydrodynamics,* 22(1), pp.58-65.

Nakatsuji, K., Yamami, H., Sueyoshi, T. and Fujiwara, T. (1992). Numerical study of the residual current in Osaka Bay, *JSCE Journal of Coastal Engineering*, 39, 906-910.

Nakayama, A. (2012). Large-eddy simulation method for flows in rivers and coasts constructed on a cartesian grid system. *Memoirs of Construction Engineering Research Institute*, 54(papers), pp.13-27.

Sharp, J. J. and Vyas, B.D. (1977). The buoyant wall jet, *Proc. Instn. Civ. Engrs.* (*London*), 63(2), 593-611.

Yokojima, S. and Nakayama, A. (2002). Filtering effects of freesurface fluctuations in LES of open-channel turbulent flows, *Annu. J. Hydraulic Engng. JSCE* 46, 379–384.